

All-optical magnetization switching in ferrimagnetic alloys: deterministic vs thermally activated dynamics

L. Le Guyader*

Helmholtz-Zentrum Berlin für Materialien und Energie GmbH,

Albert-Einstein-Strasse 15, 12489 Berlin, Germany and

Swiss Light Source, Paul Scherrer Institut, CH-5232 PSI-Villigen, Switzerland

S. El Moussaoui,[†] M. Buzzi, and F. Nolting

Swiss Light Source, Paul Scherrer Institut, CH-5232 PSI-Villigen, Switzerland

M. Savoini,[‡] A. Kirilyuk, Th. Rasing, and A. V. Kimel

Radboud University Nijmegen, Institute for Molecules

and Materials, 6525 AJ Nijmegen, The Netherlands

A. Tsukamoto and A. Itoh

College of Science and Technology, Nihon University, 24-1

Narashinodai 7-chome, Funabashi-shi, Chiba 274-8501, Japan

(Dated: March 10, 2022)

Abstract

Using photo-emission electron microscopy with X-ray magnetic circular dichroism as a contrast mechanism, new insights into the all-optical magnetization switching (AOS) phenomenon in GdFe based rare-earth transition metal ferrimagnetic alloys are provided. From a sequence of static images taken after single linearly polarized laser pulse excitation, the repeatability of AOS can be measured with a correlation coefficient. It is found that low coercivity enables thermally activated domain wall motion, limiting in turn the repeatability of the switching. Time-resolved measurement of the magnetization dynamics reveal that while AOS occurs below and above the magnetization compensation temperature T_M , it is not observed in GdFe samples where T_M is absent. Finally, AOS is experimentally demonstrated against an applied magnetic field of up to 180 mT.

PACS numbers: 75.78.Jp, 68.37.Yz, 75.70.Kw, 75.50.Gg

I. INTRODUCTION

Controlling magnetism on the ultrashort time scale of sub-100 ps has become an important research subject, not only for the potential applications in novel high density and high speed magnetic recording technologies but also for the unique opportunity to investigate magnetism on the fundamental time scales of the interactions between electrons, spins and lattice.¹ The demonstration in 1996² of a rather unexpected ultrafast sub-ps demagnetization in a thin Ni film upon femtosecond laser excitation inspired a large number of following studies.³ Of particular importance was the surprising demonstration of a deterministic magnetization reversal by the sole action of a single 40 fs laser pulse in GdFeCo rare earth-transition metal (RE-TM) alloys.⁴ The microscopic mechanism responsible for this phenomenon, now referred to as all-optical switching (AOS), remains debated. Element selective studies of the ultrafast demagnetization in GdFeCo alloys led to the interpretation that AOS is driven by the heating from the laser pulse and is therefore independent of the laser polarization and largely insensitive to any applied magnetic field.^{5,6} The helicity dependent AOS reported earlier could then be understood in terms of a differential light absorption induced by the magnetic circular dichroism in the magnetic alloy.⁷ Finally, as these RE-TM alloys usually display chemical inhomogeneities, the role of super-diffusive spin currents is also being discussed.⁸

While early studies concentrated on GdFeCo alloys, magnetization switching by laser pulses has now been reported in a growing range of systems, namely other RE-TM alloys⁹ and multi-layers,¹⁰ RE-free synthetic ferrimagnets^{10,11} and granular ferromagnets.¹² These recent developments are raising a number of crucial questions for the understanding of the AOS phenomenon and its transfer to real world applications. Among these, the exact role played by the magnetization compensation temperature T_M at which the magnetization of the two sub-lattices cancel each other remains a puzzle. On the one hand, strong changes in the magnetization dynamics upon crossing T_M have been observed¹³⁻¹⁵ and AOS seems to occur preferably for alloys displaying a T_M which can be reached through laser excitation.^{9,10,16} On the other hand, atomistic simulations of the spin dynamics as well as experiments have shown that AOS is feasible below and above T_M .⁶ In addition, helicity dependent magnetization switching in granular ferromagnets where no T_M exists has been reported.¹² Finally, in view of potential applications, it is crucial to be able to characterize to which extent AOS is a

deterministic process.

In this article, we investigate all-optical magnetization switching in GdFe based alloys using photo-emission electron microscopy (PEEM) with X-ray magnetic circular dichroism (XMCD) as a contrast mechanism, allowing imaging of the magnetic domain configuration with a spatial resolution of approximately 100 nm. Single linearly polarized laser pulses were used to excite a multi-domain configuration at temperatures below and above the magnetization compensation temperature T_M of the alloys. Introducing the Pearson product-moment correlation coefficient on series of XMCD images allows us to report a nearly purely deterministic AOS in both cases. Extrinsic pulse to pulse laser pointing stability and intrinsic finite domain sizes and thermally activated domain wall motion are found to be the main limiting factors for a purely deterministic AOS. Using time-resolved XMCD PEEM imaging of the magnetization dynamics upon femtosecond laser excitation with 70 ps time resolution and approximately 200 nm spatial resolution, it is found that AOS can even be achieved against a 180 mT applied magnetic field. Finally, strong reduction of the switching window above T_M is observed and is partly related with the proximity of the Curie temperature T_C of the sample.

II. METHODS

A. Time-resolved XMCD PEEM

In order to resolve the magnetic domain configuration and its dynamics upon AOS, the Elmitec photoemission electron microscope (PEEM) at the Surface/Interface: Microscopy (SIM) beamline¹⁷ at the Swiss Light Source (SLS) was used. Employing the X-ray magnetic circular dichroism (XMCD) effect at the Fe L_3 edge at 708 eV, a quantitative determination of the Fe spin orientation with a 100 nm spatial resolution is possible.¹⁸ From two images recorded with opposite X-ray helicity, an asymmetry image is computed which contains only normalized magnetic contrast information. Such image typically shows white or black regions corresponding to magnetic domains with magnetizations of opposite directions with respect to the X-ray propagation vector.¹⁹ Time-resolved measurements of the sample magnetization were performed by taking advantage of the pulsed nature of the X-rays produced by the SLS via the gating of the detection in synchronization to an isolated X-ray pulse. This scheme,

presented in detail in Ref. 20, allows stroboscopic pump-probe imaging of the sample with a time resolution determined by the 70 ps Full Width at Half Maximum (FWHM) temporal X-ray pulse length. At this time scale, both TM and RE magnetizations are in equilibrium such that measuring the Fe sub-lattice is sufficient to characterize the sample magnetization orientation. The pump laser pulses were produced by an XL-500 oscillator from Femtolasers Produktions GmbH which are characterized by a wavelength of $\lambda = 800$ nm, a pulse duration of $\tau = 50$ fs with an energy of 500 nJ per pulse at a 5.2 MHz repetition rate. This repetition rate is then reduced by a Pockels cell in combination with a crossed polarizer to match the 1.04 MHz repetition rate of the isolated X-ray probe pulses. The linearly p-polarized laser pump pulses were focused on the sample at a grazing incidence of 16° to a spot size of about $30 \times 100 \mu\text{m}^2$ FWHM. The time overlap ($t = 0$) between the laser and the X-ray pulse is unambiguously determined to better than ± 15 ps by the sudden space charging^{21,22} which is induced by the laser pump pulse which reduces significantly the amount of photo-emitted electrons collected by the microscope. Finally, the sample could be cooled down with a flow of liquid nitrogen and the temperature measured with a thermocouple attached to the sample holder.

B. Samples

The samples are grown on Si substrates to achieve fast cooling time during MHz repetition rate experiments²³ and are capped with a 3 nm Si_3N_4 layer to prevent oxidation. Three different samples have been used for this study. The first sample of composition Si/AlTi(10 nm)/ Si_3N_4 (5 nm)/ $\text{Gd}_{25}\text{Fe}_{65.6}\text{Co}_{9.4}$ (20 nm)/ Si_3N_4 (3 nm) has a T_M of 260 K. The two other samples are GdFe alloys of composition Si/ Si_3N_4 (5 nm)/ $\text{Gd}_{20}\text{Fe}_{80}$ (30 nm)/ Si_3N_4 (3 nm) with a T_M below 10 K and Si/ Si_3N_4 (5 nm)/ $\text{Gd}_{24}\text{Fe}_{76}$ (30 nm)/ Si_3N_4 (3 nm) with a T_M above 500 K. In the rest of the paper, each sample is referred to by a reduced notation consisting of the Gd content like for example Gd25FeCo or Gd20Fe.

III. RESULTS

A. Single laser pulse excitation

In view of potential applications, the question of the repeatability of AOS is essential. AOS was therefore studied on a multi-domain configuration where one laser pulse excites several different magnetic domains at once. The magnetic domain configuration before and after single linearly polarized laser pulse exposure was recorded with static XMCD PEEM imaging. Sequences of such I_p images taken at the Fe L_3 edge for the Gd₂₅FeCo sample at a temperature above and below T_M in the absence of any applied magnetic field are shown in Figs. 1 (a) and (c) respectively. In those images, white (black) contrast corresponds to magnetic domains whose out-of-plane magnetization has a positive (negative) projection on the X-ray direction, as indicated by the gray scale in Figs. 1 (a) and (c). In both cases, below and above T_M , changes in the magnetic domains in the center of the images are seen. To better emphasise the changes or the lack of them occurring in these multi-domains configuration, the pixel by pixel product between two successive images separated by a single linearly polarized laser pulse excitation $I_{p-1}I_p$ is computed and shown in Fig. 1(b) and (d). Irrespective of the initial magnetic domain orientation, in the $I_{p-1}I_p$ image, a black contrast corresponds to a magnetization switching (SW), a gray contrast to a domain wall (DW) and a white contrast to an absence of changes, *i.e.* no switching (NS), as indicated by the gray scale in the inset. Visible in the product of successive images $I_{p-1}I_p$ shown in Fig. 1(b) and (d) is a black elongated elliptical region at the center surrounded by a white region unaffected by the laser pulses. This elongated elliptical shape corresponds to the laser spot size seen at the 16° grazing incidence used in this experiment. This black elongated region clearly corresponds to a laser induced switching occurring equally for both magnetic domain orientations enclosed in the laser spot size. Since this AOS seems to occur with every laser pulse, it appears to be purely deterministic. To better quantify how deterministic this phenomenon of AOS really is, we introduce the pixel-by-pixel Pearson product-moment correlation coefficient r for a sequence of XMCD images as:

$$r = \frac{\sum_{p=1}^n I_{p-1}I_p}{\sqrt{\sum_{p=1}^n I_{p-1}^2} \sqrt{\sum_{p=1}^n I_p^2}},$$

where I_p is the XMCD image after p laser pulses in the sequence. In the case of purely deterministic switching, this correlation coefficient r is -1, while in the absence of changes, *i.e.* no switching, $r = +1$. In the event of an unrelated domain configuration after every single laser pulse, such as in the case of heating above T_C , $r = 0$. Such correlation coefficient images r calculated from the measured sequences are shown in Figs. 1(e) and (f) for a sample temperature above and below T_M respectively. The darkest region in these images corresponds indeed to a correlation coefficient of $r = -1$, *i.e.* a purely deterministic switching with each of the 10 laser pulse of the sequence, occurring both below and above T_M . It is also evident that the spatial extent of this $r = -1$ region is limited by the spatial extent with which these 10 laser pulses overlap. Therefore, the pulse to pulse pointing stability is the only extrinsic limitation to a somewhat purely deterministic AOS.

However, there can also be intrinsic limitation such as domain walls, in particular at the boundary between the switching and non switching region of each laser pulse. For example, in the case of the sample temperature above T_M shown in Fig. 1(b), the domain wall at the bottom of the laser pulse region is nearly continuously moving in the same direction between successive images, as indicated by the red arrows as well as the dashed ellipse in Fig. 1(e). As this domain wall is clearly outside the elongated elliptical region where AOS occurs, we know that the laser fluence is too low to induce a deterministic AOS. In fact, in the XMCD PEEM images I_1 and I_{10} shown in Fig. 1(a), one can even see the domain wall motion occurring during the imaging which results in an extended gray region rather than a either completely black or completely white region. This is indicative of a very low coercivity of the domain walls at this temperature which favors thermally activated domain wall movements in the otherwise non switching region and should be regarded as intrinsically limiting the repeatability of the AOS. Comparing the domain size above and below T_M , as shown in Figs. 1(a) and (c), one can immediately realize that the coercivity is higher in the second case as the magnetic domains are smaller, and thus more stable. Nevertheless, here some changes in the domain configuration can also be seen at the edges of the AOS region, as indicated by the blue arrow in the $I_9 I_{10}$ image shown in Fig. 1(d). The small protuberance corresponds to a small black domain outside the AOS region which disappeared between the images I_9 and I_{10} shown in Fig. 1(c). This is likely the collapse of a too small domain formed by the intersection of the existent domain pattern and the AOS region created by the laser pulse. These processes of domain collapse and thermally activated domain wall

hopping should not be confused with AOS. In fact, they lower the repeatability of AOS.

Inside the $r = -1$ region, all magnetic domains are switching with every laser pulse. However, it is unclear what is happening for the domain wall separating them since the correlation coefficient r is undefined there. To visualize the various domain wall position during the sequence of laser pulses, it is best to look at the low intensity part of the average of the squared image $\langle I_p^2 \rangle$ shown in Fig. 1(g) and (h) for the sample temperature above and below T_M , respectively. In those $\langle I_p^2 \rangle$ images, the darker the domain wall, the less it moved during the sequence of laser pulses. In the case of the sample at a temperature above T_M shown in Fig. 1(g), some changes are visible at the domain wall inside the switching region, as indicated by the red arrow. In the case below T_M shown in Fig. 1(h), no changes are visible, meaning that the domain wall stayed in place within the 100 nm spatial resolution of the instrument. Considering the low coercivity of this material, this is a rather surprising and noteworthy feature of AOS. Nevertheless, evidences for potential domain wall hopping well inside the $r = -1$ region are seen at least in one case, limiting the repeatability of the AOS. Overall, apart from the difference in coercivity, very little differences are seen between AOS below and above T_M .

B. Time-resolved dynamics around T_M

To gain more insight into the AOS and in particular into the role played by T_M , the magnetization dynamics in this sample was investigated around T_M . For this, time-resolved XMCD PEEM measurements were performed and the results are shown in Fig. 2, for a sample temperature (a) above and (c) below T_M , and for a strong $H = 180$ mT and a weak $H = 30$ mT out-of-plane magnetic field. The magnetic field is used to reset the sample magnetization to a well defined initial state, allowing for stroboscopic measurement of the dynamics. The first thing to notice is that at negative time delay t , i.e. before the laser pulse, the sample is saturated for both applied magnetic fields, and that the orientation of the Fe sub-lattice magnetization reverses between Fig. 2(a) and (c), meaning that the sample is effectively on either side of the magnetization compensation temperature T_M at the temperature used. From the time-resolved XMCD images, the magnetization dynamics at the center can be extracted and is shown in Figs. 2(b) and (d), for a sample temperature above and below T_M , respectively. In both cases, magnetization switching occurs right

after the laser pulse excites the sample. Thus, within the 70 ps time resolution of the experiments, no difference is seen in the switching dynamics for either low or high magnetic field and either below or above T_M . On the other hand, the relaxation towards the final state is strongly influenced by both the applied magnetic field and the sample base temperature. At a temperature above T_M , as shown in Fig. 2(b), the reversed state is unstable against the applied magnetic field, leading to a fast relaxation towards the initial state, the faster the higher the field. It is worth noting here that switching with a laser pulse against a field of 180 mT is thus possible, even though the relaxation is very fast, demonstrating the impetuosity by which this AOS occurs.⁶ Due to this fast relaxation and the 70 ps long X-ray probe pulse length, a saturated switched state is not observed. At temperatures below T_M as shown in Fig. 2(d), the reversed state is now stable within the illuminated area, indicating that the temperature in this region is now above T_M . In this case, after the laser pulse, the applied magnetic field is now stabilizing the reversed domain, leading to a very long life time.

Time-resolved XMCD PEEM images taken at the same fixed time delay of $t = +230$ ps after the laser pulse on the same Gd₂₅FeCo sample are shown in Fig. 3(a) above and (b) below T_M , as a function of the laser pump fluence. A small static out-of-plane magnetic field of $H = 30$ mT was applied to reset the sample after switching. This 30 mT magnetic field is small enough to not hinder the AOS at this time scale as can be seen in Fig. 2(b). While below T_M , the laser fluence can be increased significantly without losing the AOS, the same is not true above T_M . There, a small 10% increase from 2.7 to 3.0 mJ·cm⁻² is enough to bring the central region of the laser spot into a demagnetized state. This effect is most striking at the fluence of $\mathcal{F} = 3.5$ mJ·cm⁻² in Fig. 3(a), where the switched region forms a very thin 2 μ m wide ring around the laser pulse. The AOS fluence switching window is thus reduced above T_M , and this asymmetry of the switching window around T_M is consistent with literature.¹³⁻¹⁵ Part of this effect might be attributed to the proximity with the Curie temperature T_C .

C. Time-resolved dynamics far from T_M

Due to the limited accessible temperature range in the PEEM, investigation of the AOS far from T_M requires samples with different compositions. For this, time-resolved XMCD

PEEM measurement were thus performed on Gd20Fe with T_M around 0 K and Gd24Fe with T_M around 500 K, under a small static out-of-plane magnetic field of 30 mT. The results are shown in Fig. 4. For both samples, a time resolution limited demagnetization process occurs. The samples then stay demagnetized for about 500 ps which is then followed by a slow dynamics on a time scale of around 10 ns, towards the initial state for Gd20Fe and towards the reversed state for Gd24Fe. This reversal in the Gd24Fe sample shows that there is an accessible magnetization compensation temperature T_M in this sample below T_C , allowing the applied 30 mT out-of-plane magnetic field to reverse the sample magnetization on a slow few nanoseconds long time scale and eventually back to the initial state at even longer time scale after cooling down. For the Gd20Fe sample, the temperature is already above T_M before the laser pulse, and therefore no magnetic field assisted switching occurs. Looking at the XMCD PEEM images taken at fix time delay and shown in Fig. 4(a), it can be seen that in the case of the Gd20Fe sample, the demagnetized region has a diffuse boundary, meaning that no magnetic domain is actually formed. On the other hand, for Gd24Fe, at around 750 ps after the laser pulse, a clear boundary appears in the heated region, which is seen in Fig. 4(a) at $t = 3.1$ ns. This very late formation of the reversed domain in Gd24Fe and the absence of switching in Gd20Fe allow us to conclude that no AOS window exists far from T_M .

IV. DISCUSSION

Determining if a system can display all-optical magnetization switching and to which extent this AOS is deterministic are two questions of crucial importance, for a better understanding of the phenomenon as well as in view of its potential applications. In this context, sequences of XMCD PEEM images separated by single linearly polarized laser pulse excitation on a multi-domain configuration such as shown in Fig.1 can provide valuable information. First of all, since linearly p-polarized laser pulses are equally absorbed by each domain orientation, a direct comparison between what happens inside each domain is possible.⁷ This is in contrast with multiple circularly polarized laser pulses used in recent studies such as in Refs. 10 and 12, where such a comparison can only be made after carefully taking into account the magnetic circular dichroism of the material. Second, randomly demagnetized initial states are better than saturated or artificially created domain states

since no stray field is created which could influence the switching. Third, the reversed domain configuration in such case is known to be stable as well, therefore a collapse of the reversed domain state because of too low coercivity or too high net magnetization is not to be expected.²⁴ Finally, from such a sequence of images, the actual reproducibility of AOS can be measured using the Pearson product-moment correlation coefficient r as introduced.

From our analysis, it follows that the purely deterministic AOS observed in the GdFeCo samples is limited by a number of extrinsic and intrinsic effects. The largest limitation we observe in Fig. 1(e) and (f) is the pulse to pulse laser pointing stability which is extrinsic in nature to the switching phenomenon itself. The second limitation observed is related to the stability of the domain configuration. For example, at the edge of the laser pulse, the overlap of the $r = -1$ switching region with the preexistent domain configuration can create domains which are too small to be stable, as seen in Fig. 1(d) I_9I_{10} . In addition, thermal activation of domain walls can occur outside as well as inside the $r = -1$ switching region, as seen in Fig. 1(g) and indicated by the arrow and dashed ellipse. Since these two effects are related to the coercivity of the material, this constitutes an intrinsic limitation to the repeatability of the AOS. However, by understanding these limitations, we can envisage that engineered materials can potentially alleviate these limitations. For example, in patterned materials where each structure preferably host a single magnetic domain, a purely deterministic switching would be maintained.

Regarding the role played by the magnetization compensation temperature T_M on the AOS, we first of all confirm previous studies in that AOS occurs below and above T_M .^{6,14} Single shot laser pulse experiments shown in Fig. 1 as well as time-resolved measurements of the magnetization dynamics shown in Fig. 2 both reveal AOS below as well as above T_M . However, there exists a clear difference between switching below and above T_M , as shown in the fluence-dependent patterns observed at $t = 230$ ps in Fig. 3. In addition, for GdFe samples with no or far from their T_M , no switching is observed, as shown in Fig. 4. This leads to the conclusion that while the existence of a reachable T_M during the laser excitation is not a strict requirement to observe AOS, sample compositions with T_M near room temperature are preferred. It must be noted that in addition to T_M , an angular momentum compensation temperature T_A also exists at a slightly higher temperature.²⁵ However, our experimental geometry with out-of-plane magnetic field does not allow magnetization precession dynamics to be observed, precluding any investigation of the effect of T_A on AOS. Finally, AOS is a

very robust switching mechanism as it can be realized against an opposing applied magnetic field⁶, as demonstrated experimentally here in the case of a 180 mT field in Fig. 2(b).

V. CONCLUSIONS

In conclusion, using static and time-resolved PEEM microscopy with XMCD to probe the sample magnetization upon laser excitation, important aspects of the AOS have been revealed. Sequences of images after single linearly polarized laser pulse excitation on a multi-domain configuration allow for the study of the repeatability of the process by using the correlation coefficient as its measure. It is found the AOS in the Gd₂₅FeCo sample studied is nearly purely deterministic. Moreover, intrinsic limitation from the low coercivity of the material leading to thermally activated domain wall hopping could be alleviated in patterned media. From the time-resolved measurement of the magnetization dynamics, it is found that AOS occurs below and above T_M , while on the other hand, no AOS occurs for sample temperatures far from it. Strong reduction of the fluence switching window occurs above T_M and is likely related to the proximity with the Curie temperature T_C . Finally, AOS against an applied magnetic field of 180 mT is demonstrated, illustrating the impetus by which AOS occurs.

ACKNOWLEDGMENTS

We thank the European Research Council under the European Unions Seventh Framework Programme FP7/2007–2013 (grants NMP3-SL-2008-214469 (UltraMagnetron), FP7-NMP-2011-SMALL- 281043 (FEMTOSPIN) and 214810 (FANTOMAS)) for part of the financial supports as well as the MEXT-Supported Program for the Strategic Research Foundation at Private Universities, 2013–2017. Part of this work was performed at the Swiss Light Source, Paul Scherrer Institut, Villigen, Switzerland. We thank J. Honegger for his support.

* email: loic.le.guyader@helmholtz-berlin.de

- [†] Present address: College of Science and Technology, Nihon University, 24-1 Narashinodai 7-chome, Funabashi-shi, Chiba 274-8501, Japan
- [‡] Present address: Institute for Quantum Electronics, Physics Department, ETH Zurich, CH-8093 Zurich, Switzerland
- ¹ J. Stöhr and H. C. Siegmann, *Magnetism: From Fundamentals to Nanoscale Dynamics* (Springer-Verlag, Berlin Heidelberg, 2006).
- ² E. Beaurepaire, J.-C. Merle, A. Daunois, and J.-Y. Bigot, “Ultrafast spin dynamics in ferromagnetic nickel,” *Phys. Rev. Lett.* **76**, 4250–4253 (1996).
- ³ Andrei Kirilyuk, Alexey V. Kimel, and Theo Rasing, “Ultrafast optical manipulation of magnetic order,” *Rev. Mod. Phys.* **82**, 2731–2784 (2010).
- ⁴ C. D. Stanciu, F. Hansteen, A. V. Kimel, A. Kirilyuk, A. Tsukamoto, A. Itoh, and Th. Rasing, “All-optical magnetic recording with circularly polarized light,” *Phys. Rev. Lett.* **99**, 047601 (2007).
- ⁵ I. Radu, K. Vahaplar, C. Stamm, T. Kachel, N. Pontius, H. A. Dürr, T. A. Ostler, J. Barker, R. F. L. Evans, R. W. Chantrell, *et al.*, “Transient ferromagnetic-like state mediating ultrafast reversal of antiferromagnetically coupled spins,” *Nature* **472**, 205–208 (2011).
- ⁶ T. A. Ostler, J. Barker, R. F. L. Evans, R. Chantrell, U. Atxitia, O. Chubykalo-Fesenko, S. El Moussaoui, L. Le Guyader, E. Mengotti, L. J. Heyderman, *et al.*, “Ultrafast heating as a sufficient stimulus for magnetization reversal in a ferrimagnet,” *Nat. Commun.* **3**, 666 (2012).
- ⁷ A. R. Khorsand, M. Savoini, A. Kirilyuk, A. V. Kimel, A. Tsukamoto, A. Itoh, and Th. Rasing, “Role of magnetic circular dichroism in all-optical magnetic recording,” *Phys. Rev. Lett.* **108**, 127205 (2012).
- ⁸ C. E. Graves, A. H. Reid, T. Wang, B. Wu, S. de Jong, K. Vahaplar, I. Radu, D. P. Bernstein, M. Messerschmidt, L. Müller, R. Coffee, M. Bionta, S. W. Epp, R. Hartmann, N. Kimmel, G. Hauser, A. Hartmann, P. Holl, H. Gorke, J. H. Mentink, A. Tsukamoto, A. Fognini, J. J. Turner, W. F. Schlotter, D. Rolles, H. Soltau, L. Strüder, Y. Acremann, A. V. Kimel, A. Kirilyuk, Th. Rasing, J. Stöhr, A. O. Scherz, and H. A. Dürr, “Nanoscale spin reversal by non-local angular momentum transfer following ultrafast laser excitation in ferrimagnetic GdFeCo,” *Nat. Mater.* (2013), 10.1038/nmat3597.
- ⁹ Sabine Alebrand, Matthias Gottwald, Michel Hehn, Daniel Steil, Mirko Cinchetti, Daniel Lacour, Eric E. Fullerton, Martin Aeschlimann, and Stéphane Mangin, “Light-induced magneti-

- zation reversal of high-anisotropy TbCo alloy films,” *Appl. Phys. Lett.* **101**, 162408 (2012).
- ¹⁰ S. Mangin, M. Gottwald, C-H. Lambert, D. Steil, V. Uhlíř, L. Pang, M. Hehn, S. Alebrand, M. Cinchetti, G. Malinowski, *et al.*, “Engineered materials for all-optical helicity-dependent magnetic switching,” *Nature Mater.* **13**, 286–292 (2014).
- ¹¹ Richard F. L. Evans, Thomas A. Ostler, Roy W. Chantrell, Ilie Radu, and Theo Rasing, “Ultrafast thermally induced magnetic switching in synthetic ferrimagnets,” *Appl. Phys. Lett.* **104**, 082410 (2014).
- ¹² C-H. Lambert *et al.*, “All-optical control of ferromagnetic thin films and nanostructures,” *Science* **345**, 1337 (2014).
- ¹³ K. Vahaplar, A. M. Kalashnikova, A. V. Kimel, D. Hinzke, U. Nowak, R. Chantrell, A. Tsukamoto, A. Itoh, A. Kirilyuk, and Th. Rasing, “Ultrafast path for optical magnetization reversal via a strongly nonequilibrium state,” *Phys. Rev. Lett.* **103**, 117201 (2009).
- ¹⁴ K. Vahaplar, A. M. Kalashnikova, A. V. Kimel, S. Gerlach, D. Hinzke, U. Nowak, R. Chantrell, A. Tsukamoto, A. Itoh, A. Kirilyuk, and Th. Rasing, “All-optical magnetization reversal by circularly polarized laser pulses: Experiment and multiscale modeling,” *Phys. Rev. B* **85**, 104402 (2012).
- ¹⁵ R. Medapalli, I. Razdolski, M. Savoini, A. R. Khorsand, A. Kirilyuk, A. V. Kimel, Th. Rasing, A. M. Kalashnikova, A. Tsukamoto, and A. Itoh, “Efficiency of ultrafast laser-induced demagnetization in $\text{Gd}_x\text{Fe}_{100-x-y}\text{Co}_y$ alloys,” *Phys. Rev. B* **86**, 054442 (2012).
- ¹⁶ Sabine Alebrand, Alexander Hassdenteufel, Daniel Steil, Marianne Bader, Alexander Fischer, Mirko Cinchetti, and Martin Aeschlimann, “All-optical magnetization switching using phase shaped ultrashort laser pulses,” *physica status solidi (a)* **209**, 2589–2595 (2012).
- ¹⁷ U. Flechsig, F. Nolting, A. Fraile Rodríguez, J. Krempaský, C. Quitmann, T. Schmidt, S. Spielmann, and D. Zimoch, “Performance measurements at the SLS SIM beamline,” *AIP Conf. Proc.* **1234**, 319–322 (2010).
- ¹⁸ F. Nolting, “Magnetism and synchrotron radiation,” (Springer-Verlag, Berlin Heidelberg, 2010) Chap. Magnetic Imaging with X-rays, p. 345.
- ¹⁹ Andreas Scholl, Hendrik Ohldag, Frithjof Nolting, Joachim Stöhr, and Howard A. Padmore, “X-ray photoemission electron microscopy, a tool for the investigation of complex magnetic structures (invited),” *Rev. Sci. Instrum.* **73**, 1362–1366 (2002).

- ²⁰ L. Le Guyader, Armin Kleibert, Arantxa Fraile Rodríguez, Souliman El Moussaoui, Ana Balan, Michele Buzzi, J. Raabe, and Frithjof Nolting, “Studying nanomagnets and magnetic heterostructures with X-ray PEEM at the Swiss Light Source,” *Journal of Electron Spectroscopy and Related Phenomena* **185**, 371 – 380 (2012).
- ²¹ A. Mikkelsen, J. Schwenke, T. Fordell, G. Luo, K. Klunder, E. Hilner, N. Anttu, A. A. Zakharov, E. Lundgren, J. Mauritsson, *et al.*, “Photoemission electron microscopy using extreme ultraviolet attosecond pulse trains,” *Rev. Sci. Instrum.* **80**, 123703 (2009).
- ²² N M Buckanie, J Göhre, P Zhou, D. von der Linde, M. Horn-von Hoegen, and F-J. Meyer zu Heringdorf, “Space charge effects in photoemission electron microscopy using amplified femtosecond laser pulses,” *J. Phys.: Condens. Matter* **21**, 314003 (2009).
- ²³ Alexander Hassdenteufel, Christian Schubert, Birgit Hebler, Helmut Schultheiss, Jürgen Fassbender, Manfred Albrecht, and Rudolf Bratschitsch, “All-optical helicity dependent magnetic switching in Tb-Fe thin films with a MHz laser oscillator,” *Opt. Express* **22**, 10017–10025 (2014).
- ²⁴ C. Schubert, A. Hassdenteufel, P. Matthes, J. Schmidt, M. Helm, R. Bratschitsch, and M. Albrecht, “All-optical helicity dependent magnetic switching in an artificial zero moment magnet,” *Appl. Phys. Lett.* **104**, 082406 (2014).
- ²⁵ C. D. Stanciu, A. V. Kimel, F. Hansteen, A. Tsukamoto, A. Itoh, A. Kirilyuk, and Th. Rasing, “Ultrafast spin dynamics across compensation points in ferrimagnetic GdFeCo: The role of angular momentum compensation,” *Phys. Rev. B* **73**, 220402 (2006).

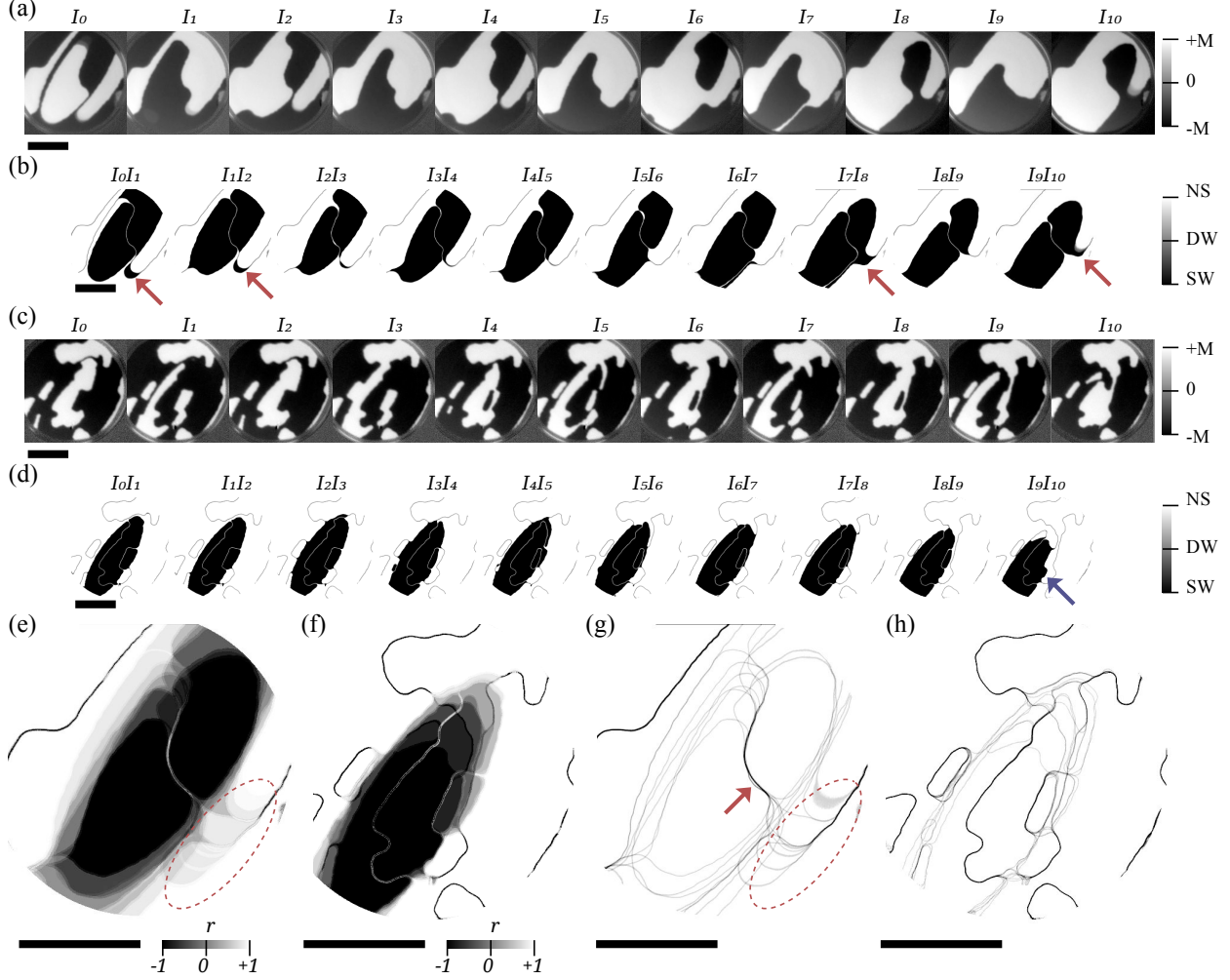


FIG. 1. (Color online)(a) Sequences of XMCD PEEM images I_p taken after p single laser pulse excitation above at $T = 300$ K and (c) below at $T = 160$ K the magnetization compensation temperature $T_M = 260$ K of the Gd₂₅FeCo sample. The gray scale in the inset on the right indicates the out-of-plane magnetization orientation. (b) Sequences of image product $I_{p-1}I_p$ above and (d) below T_M . The gray scale in the inset on the right indicates which gray level corresponds to magnetization switching (SW), no switching (NS) or domain wall (DW).(e) Correlation coefficient images r derived from the sequences of single laser pulse excitation above and (f) below T_M . (g) Average image $\langle I_p^2 \rangle$ showing the domain wall positions above and (h) below T_M . Arrows and dashed ellipses indicate magnetization switching not related to AOS and are discussed in the text. All scale bars are $20 \mu\text{m}$.

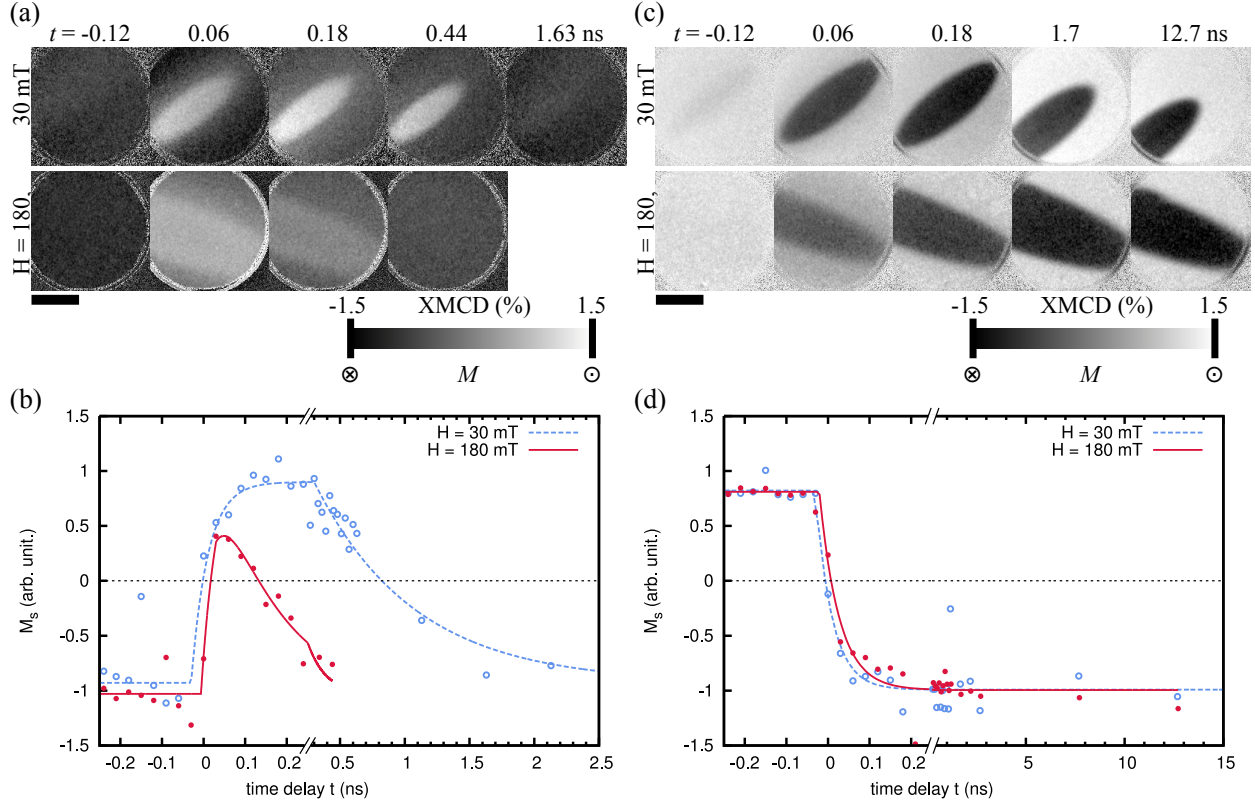


FIG. 2. (Color online)(a) Time-resolved XMCD PEEM images on Gd₂₅FeCo sample at different time delays, for two different applied out-of-plane magnetic field of 30 mT and 180 mT, measured at the Fe L₃ edge, at a temperature above T_M at $T = 300$ K and (b) the extracted magnetization dynamics for each applied out-of-plane magnetic field. (c) and (d) the same for a sample temperature below T_M at $T = 160$ K. The scale bars are $20 \mu\text{m}$.

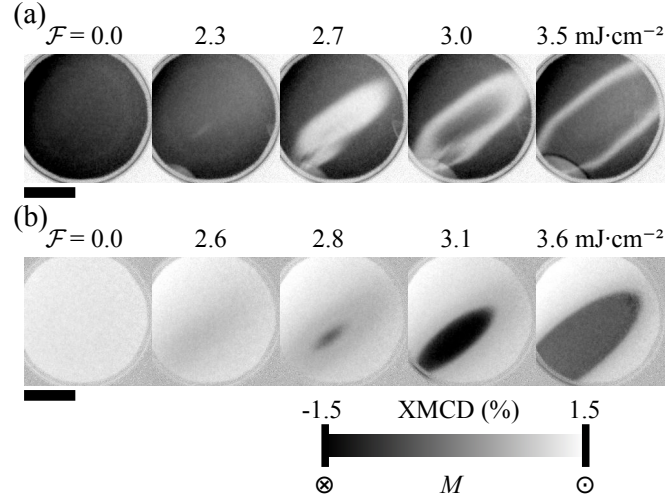


FIG. 3. (a) Time-resolved XMCD PEEM images taken at $t = 230$ ps after the laser pulse on Gd₂₅FeCo sample above at $T = 300$ K and (b) below at $T = 160$ K the magnetization compensation temperature $T_M = 260$ K, as a function of the laser pump fluence. The static out-of-plane magnetic field was 30 mT. The scale bars are $20 \mu\text{m}$.

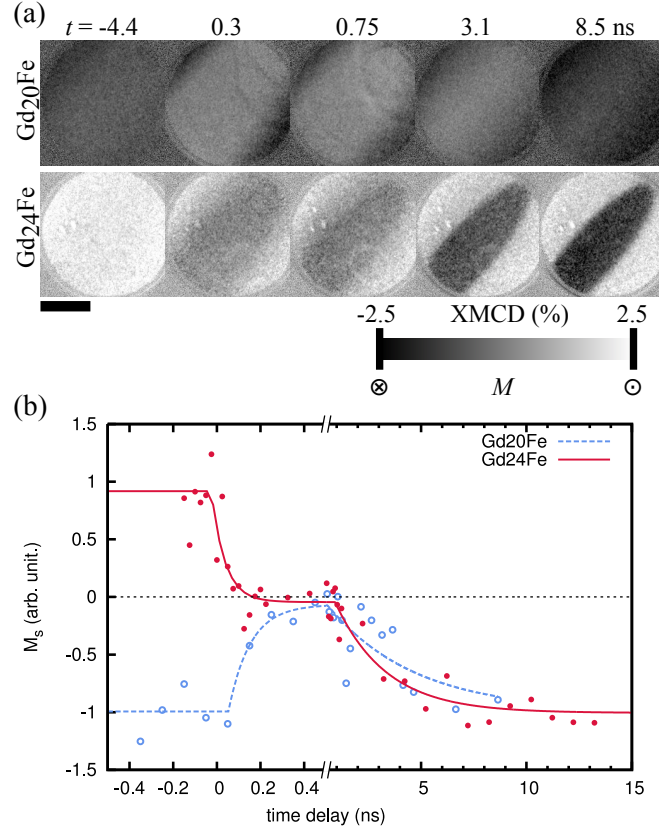


FIG. 4. (Color online)(a) Time-resolved XMCD PEEM images at various fixed time delays and (b) extracted magnetization dynamics on Gd₂₀Fe (T_M around 0 K, $\mathcal{F} = 5.7$ mJ·cm⁻²) and Gd₂₄Fe (T_M around 500 K, $\mathcal{F} = 3.9$ mJ·cm⁻²) samples at room temperature with a 30 mT of out-of-plane magnetic field. The scale bar is 20 μ m.